

# Hot Gas in High-Redshift Protogalaxies: Observations of High-Ion Absorption in Damped Lyman-Alpha Systems

Andrew J. Fox<sup>1</sup>  
 Patrick Petitjean<sup>1,2</sup>  
 Cédric Ledoux<sup>3</sup>  
 Raghunathan Srianand<sup>4</sup>

<sup>1</sup> Institut d'Astrophysique de Paris,  
 Université Pierre et Marie Curie, Paris,  
 France

<sup>2</sup> LERMA, Observatoire de Paris, France

<sup>3</sup> ESO

<sup>4</sup> Inter-University Centre for Astronomy  
 and Astrophysics – IUCAA, Ganesh  
 Khind, Pune, India

The neutral discs of high-redshift galaxies give rise to the Damped Lyman- $\alpha$  (DLA) systems seen in the spectra of background quasars. We show for the first time that a hot phase of gas is present in DLAs, observable in the absorption lines of five-times-ionised oxygen. This plasma phase, which could harbour a considerable fraction of all the metals produced by star formation at these epochs, can be explained as the feedback from star formation taking place in the neutral discs.

## Studying galaxy halos at high redshift

To obtain observations of galaxies at high redshift, one can pursue deep imaging in the optical and infrared, or look for absorption-line signatures in the spectra of background QSOs. These two methods are complementary, but whereas direct imaging is biased towards bright objects, absorption lines select galaxies irrespective of brightness. If the sight line toward a particular QSO intersects the neutral disc of a galaxy, a Damped Lyman- $\alpha$  (DLA) absorption system will be observed in the quasar spectrum. This name reflects the strong damping wings of the Lyman- $\alpha$  transition seen in these systems. Observationally, DLAs are defined as those QSO absorbers with H I column densities  $N(\text{H I}) > 2 \times 10^{20} \text{ cm}^{-2}$ . Those absorbers with slightly lower H I column densities (between  $10^{19}$  and  $2 \times 10^{20} \text{ cm}^{-2}$ ) are referred to as sub-DLAs. DLAs represent the largest reservoirs of neutral gas (and hence fuel for star formation) in the redshift range 0–5 (see review by Wolfe et al. 2005). Since the advent of 10-m-class telescopes, the chemical con-

tent of DLAs and sub-DLAs at high redshift has been carefully studied, providing a means to trace the process of cosmic metal enrichment over a large fraction of the age of the Universe.

We recently began a programme to look for a hot ionised medium in DLAs and sub-DLAs. Two separate processes could create such a medium, we reasoned. If DLAs do represent high-redshift galaxies, then star formation and subsequent Type II supernova explosions will create super-bubbles of hot, shock-heated interstellar plasma. Sufficiently powerful supernovae can drive winds that enrich the surrounding intergalactic medium with metals. The separate process of accretion and shock-heating of infalling intergalactic gas could also lead to the production of a hot ionised medium, though this process is predicted to be less important at high redshift: hydrodynamical simulations have shown that the fraction of all baryons in the temperature range  $10^5$  to  $10^7 \text{ K}$  rises from a few per cent at  $z = 3$  to  $\approx 30\%$  at  $z = 0$  (Davé et al. 2001).

The ultraviolet (UV) lines available for studying highly ionised interstellar plasma are the O VI  $\lambda\lambda$  1031, 1037, N V  $\lambda\lambda$  1238, 1242, C IV  $\lambda\lambda$  1548, 1550, and Si IV  $\lambda\lambda$  1393, 1402 Å doublets. O VI, which traces gas in the temperature range  $10^{5-6} \text{ K}$ , is of particular interest since it is the most highly ionised of all the species with UV lines. Furthermore, oxygen is the third most abundant element in the Universe (after hydrogen and helium), and the O VI lines are intrinsically strong, rendering them easy to observe. O VI systems are only accessible from the ground at  $z > 2$ , where the transitions become redshifted enough to pass the atmospheric cut-off near 300 nm.

## Observations and sample selection

A large data set of DLA spectra has been built up using the Ultraviolet-Visual Echelle Spectrograph (UVES) on VLT UT2 in the years 2000 to 2006. The data set currently consists of 123 DLAs and sub-DLAs. We formed two subsamples from the data: all the DLAs with detections in the C IV line, and all the DLAs with detections in O VI. The C IV sample, containing 73 systems, is larger since the lines lie

redward of the Lyman- $\alpha$  forest and so are subject to a much lower level of contamination. The O VI sample is much smaller (12 systems), since in many cases the O VI lines are blended with the Lyman- $\alpha$  forest, the series of intervening H I absorption lines found at wavelengths shortward of the quasar's Lyman- $\alpha$  emission line. We dealt with the confusion of separating O VI from H I interlopers by adopting a series of systematic steps to identify genuine DLA O VI absorbers. These steps included verifying the doublet ratio between the two O VI lines, and checking to see whether candidate O VI identifications could be caused by intervening Lyman- $\alpha$ , Lyman- $\beta$ , or Lyman- $\gamma$  forest absorbers, by looking in each case for corresponding absorption in the other Lyman series lines. We detect O VI in 12 of 35 DLAs (34 %) with O VI coverage. In the remaining 66 % of cases, we cannot tell whether O VI is present or not due to the blending. Thus a conservative estimate of the fraction of DLAs with O VI is  $> 34\%$ . N V is detected in 3/9 systems with data covering the appropriate wavelength range.

## Example of DLA spectra

In Figure 1 we show the absorption line profiles of three example DLA systems with O VI detections. Within each column of this figure we show a Si II or Fe II line chosen to trace the neutral gas, together with all the available high ionisation data. Our model fits are included on the plot in red. We do not include all the spectra here: the full spectra are available in Figure 1 in Fox et al. (2007a). There is considerable variation in the appearance of the highly ionised absorption lines in the DLAs. The O VI absorbers range from cases with a single, optically thin component to cases with a series of saturated components. The C IV profiles range from cases with one or two components spanning  $< 100 \text{ km s}^{-1}$  to cases with over 15 components spanning several hundred  $\text{km s}^{-1}$ . It is interesting to note that the mean integrated O VI column density in our 12 detections,  $\log N(\text{O VI}) = 14.54$ , is of similar order to the mean O VI column density seen in the halo of the Milky Way, even though the metallicities of the DLAs in our sample are typically only one-fortieth of the solar value. This implies that the total ionised hydrogen column densi-

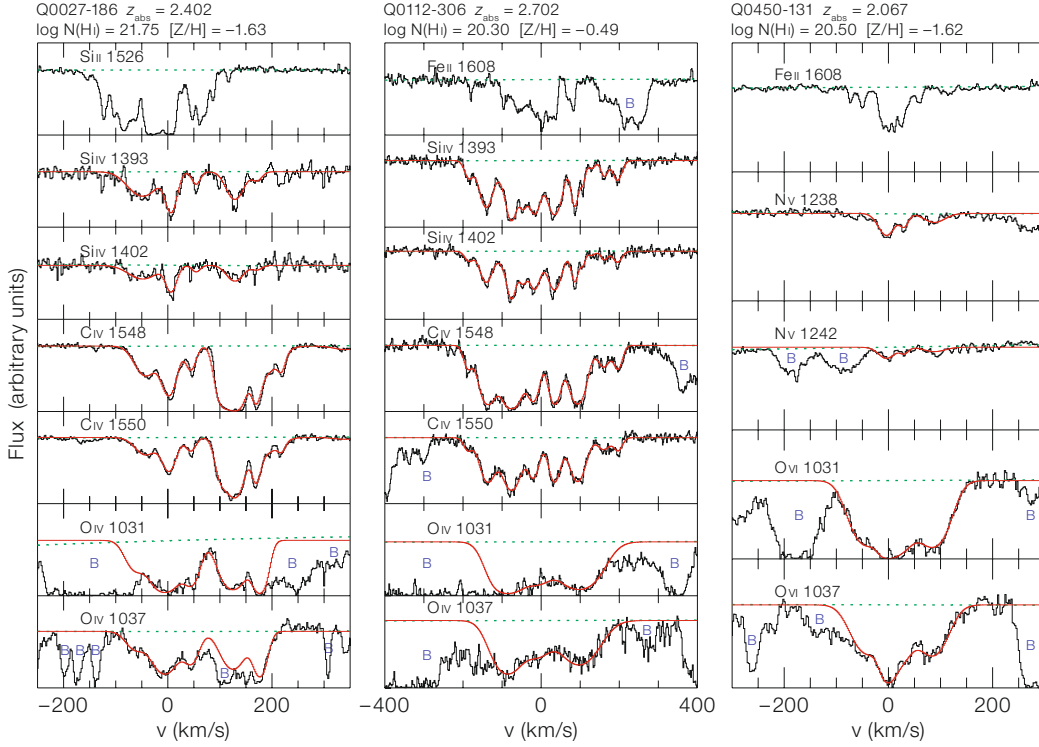


**Figure 1:** VLT/UVES absorption-line spectra of three example DLA systems with detections of O VI absorption. The tracer of the neutral gas is shown in the top panel, with the other panels showing all available high-ionisation data. In each DLA  $v = 0$  km/s is defined by the redshift annotated at the top of the column, which corresponds to the strongest component of absorption in the neutral gas. The red line shows our VPFIT model of the absorption, and fitted continua are shown as light dashed lines. Blends are identified with the letter 'B'.

ties are much higher in DLAs than in the Milky Way.

### Gas temperature

In each DLA, the absorption line profiles of each high-ionisation line usually consist of several individual components. Using the freely available VPFIT software package, we determined the properties of each individual component for the O VI sample. In Figure 2 we show the distributions of the component line width, and compare the results for O VI, C IV, and Si IV. These distributions offer information on the physical conditions in the absorbing gas.

Many of the C IV and Si IV components in DLAs have narrow line widths ( $b < 10$  km s<sup>-1</sup>) implying that the kinetic temperature in the gas is too low to produce the high ionisation by collisions with electrons. Instead, these components must be photoionised, by extreme-ultraviolet (EUV) photons in the extragalactic background radiation from quasars and galaxies, and potentially also from local sources of radiation. However, no individual narrow photoionised O VI components are found in the data; the narrowest

O VI  $b$ -value is 14 km s<sup>-1</sup>, with the majority of cases over 20 km s<sup>-1</sup>. This suggests that the plasma has a multi-phase structure, with the O VI arising in a hot, collisionally ionised phase, and the narrow C IV components arising in cooler clouds, which may be embedded in the hot phase.

### Evidence for star formation

We find that the bulk properties of the plasma depend strongly on the metallicity of the neutral gas. This is revealed by the detection of correlations between  $[Z/H]$  and: (1), C IV column density; (2) total C IV line width; and (3), maximum C IV velocity. These correlations are shown in Figure 3.

Similar trends are found with O VI, but we display the C IV results since the sample sizes are much larger and the correlations are more significant. We interpret these correlations as providing evidence for star formation in the DLA host galaxies. In this picture, star formation in the neutral DLA discs will lead to EUV radiation from hot stars that can photoionise carbon in the galaxy's interstellar medium (ISM) to the triply-ionised state, giving rise to the narrow C IV lines. Star formation also leads to supernovae, resulting in: (i) the release of metals generated by stellar nucleosynthesis; (ii) the production of superbubbles containing million-degree plasma, that can interact with cool or warm clouds to produce gas at temperatures where triply-ionised carbon and

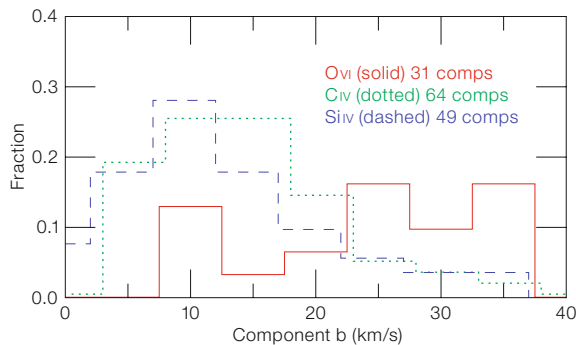


**Figure 2:** Normalised histograms of the widths of the high-ionisation components that comprise the DLA absorbers, as measured using the VPFIT component-fitting software package. The number of components in each sample is indicated on the plot. Note that  $\bar{b}(\text{Si IV}) < \bar{b}(\text{C IV}) < \bar{b}(\text{O VI})$ , i.e. the average component width rises with ionisation potential.

five-times-ionised oxygen are created through electron collisions, giving rise to the broad C IV and O VI lines; and (iii) the deposition of mechanical energy into the surrounding ISM, that imparts the large velocity dispersion to the highly-ionised components.

Our C IV line width/metallicity correlation closely follows the observed correlation between the low-ionisation line width and metallicity (Ledoux et al. 2006) which has been taken to imply an underlying mass-metallicity relation. This is because the low-ionisation line width is thought to be dominated by gravity, and hence can be used to indicate the galaxy mass. If this is true, one expects that the more metal-rich galaxies will reside in deeper potential wells, so that their ionised outflows do not become winds and escape, but rather are decelerated and exist in gravitationally-bound halos. Indeed, this mechanism has been suggested to be the origin of the mass-metallicity relation. However, we detect C IV outflows in DLAs at all values of  $[Z/H]$ , as shown in the bottom panel of Figure 3. The maximum outflow velocities reach over  $500 \text{ km s}^{-1}$  in eight high-metallicity systems. This indicates that some mechanism is capable of driving galactic winds even out of the deepest potential wells.

#### Total ionised column density

By making corrections for ionisation and for metallicity, we can convert, for each absorber, the measured O VI and C IV column densities to H II column densities. The ionisation corrections are derived from models, and the metallicities have been measured in Ledoux et al. (2006). We assume that the neutral, warm, and hot phases all share the same common metallicity, and further that the relative elemental abundances are in their solar ratios. When the hot hydrogen column densities are computed, the numbers are strikingly large. We find  $\log N(\text{H II})$  in the O VI phase ranges from  $> 19.5$  to  $> 21.1$ , and  $\log N(\text{H II})$  in the C IV phase ranges from  $> 18.4$  to  $> 20.9$ . These lower limits are typically on the same order as the H I column in the neutral gas, although we observe a considerable dispersion (over two orders of magnitude) in the value of  $N(\text{H II})/N(\text{H I})$ .

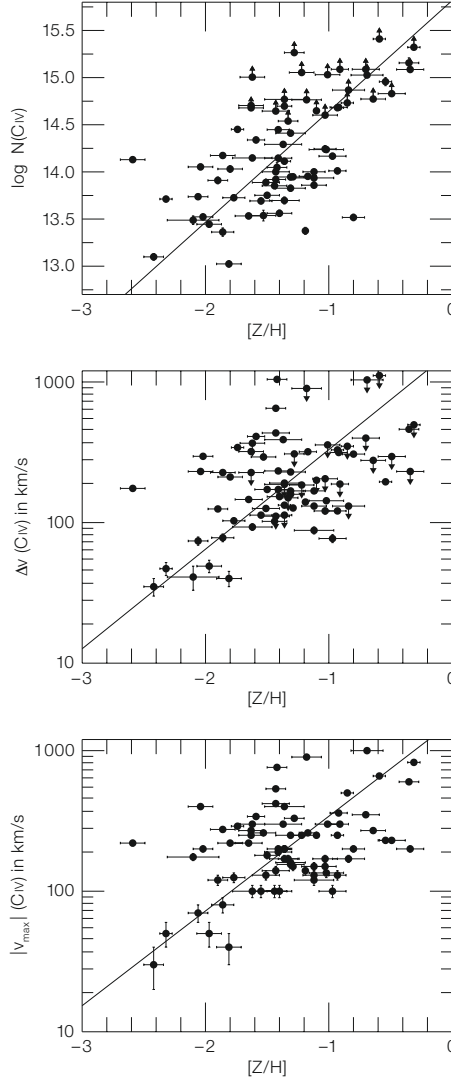


**Figure 3:** Correlations between metallicity and (1) high ionisation species column density (top panel,  $> 6 \sigma$  significance), (2) high ionisation line width (middle panel, at  $3.4 \sigma$  significance), and (3) maximum outflow velocity (bottom panel, at  $3.1 \sigma$  significance), in a sample of 73 DLAs and sub-DLAs. The metallicity is measured in the neutral phase of the gas. The solid lines show linear least-squares bisector fits to the data.

#### Contribution to $\Omega$

The contribution of H I in DLAs to the cosmic density has been calculated as  $\approx 1 \times 10^{-3}$ , fairly flat with redshift (Prochaska et al. 2005). By making use of our new estimates for the amount of ionised gas that accompanies the neutral gas in DLAs, we can compute the contribution of the hot gas in DLAs to the closure density. This calculation has the advantage of not depending on the distribution of gas

within the DLA halos. When using our median values  $N(\text{H II, Hot})/N(\text{H I}) > 0.4$  and  $N(\text{H II, Warm})/N(\text{H I}) > 0.1$ , we find that the contribution from the hot and warm ionised phases in DLAs to  $\Omega$  is  $> 4 \times 10^{-4}$  and  $> 1 \times 10^{-4}$ , respectively. These numbers are small compared to the total density of baryons, since at  $z > 2$  the majority of the baryons are thought to lie in the diffuse Lyman- $\alpha$  forest (Rauch et al. 1998).

#### Missing metals

Although the DLAs are unimportant in the baryon budget at high redshift, they may play a significant role in the metal budget. The total amount of metals released by  $z = 2$  can be calculated by integrating the observed star-formation history of the Universe, and using the metal yields from models of stellar nucleosynthesis. Using the star-formation rate from Bouwens et al. (2004), the resulting number expressed in units of the critical density is  $\Omega_{\text{Z}}^{\text{SFH}} \approx 3 \times 10^{-5}$ . Stars in galaxies appear to contain  $\approx 20\%$  of the total, the contribution from the ISM in galaxies (H I in DLAs) is  $\sim 1\%$ , and the IGM contains a further  $\approx 5\text{--}25\%$ . The remaining metals ( $\approx 50\%$  of the total) are yet to be found, leading to a situation referred to as the “missing metal problem” (Bouché et al. 2007, and references therein). Hot, low-metallicity, low-density gas is a possible solution to the missing metals problem. For plasma with a density of  $10^{-3} \text{ cm}^{-3}$ , a metallicity of 0.01 solar, and a temperature of  $10^6 \text{ K}$ , we calculate the cooling time to be  $\approx 12$  billion years, i.e. approximately the Hubble time, showing that gas and metals can become essentially locked up in hot halos.

If  $f(\text{O VI})$  in the DLA plasma were as low as  $3 \times 10^{-3}$ , which is the case for plasma in collisional ionisation equilibrium at  $10^6 \text{ K}$  (Gnat and Sternberg 2007), then the O VI-bearing plasma around DLAs would contain enough metals to solve the missing metals problem. The widths of the broader O VI lines in our sample are consistent with the thermal broadening expected at  $10^6 \text{ K}$ . However, since metals will also be found in both the neutral and ionised phases of other categories of quasar absorption line system, it is unlikely that  $f(\text{O VI})$  will take a value as low



as  $3 \times 10^{-3}$ . These other categories include the low H I column density absorbers known as Lyman Limit Systems, which may probe the remotest regions of galactic halos. Further studies are needed to search for and characterise the O VI phase in QSO absorbers over all ranges of N(H I), in order to fully measure the quantity of baryons and metals hidden in hot galactic halos at high redshift.

We conclude by noting that if  $10^6$  K gas is present in DLAs, the majority of oxygen atoms will be ionised up to O VII and O VIII. The resonance lines of these ions are in the X-ray, but unfortunately searches

for O VII and O VIII absorption in DLAs to confirm the presence of  $10^6$  K plasma are beyond the capabilities of current X-ray satellites, and must wait for a new generation of X-ray satellites (*XEUS*, *Constellation-X*).

#### Acknowledgements

Andrew J. Fox gratefully acknowledges support from a Marie Curie Intra-European Fellowship awarded by the European Union Sixth Framework Programme. We have made use of the VPFIT software package, written by Bob Carswell and available at <http://www.ast.cam.ac.uk/rfc/vpfrit.html>. Patrick Petitjean and Raghunathan Srikanth gratefully acknowledge support from the Indo-French Centre for the Promotion

of Advanced Research (Centre Franco-Indien pour la Promotion de la Recherche Avancée) under contract No. 3004-3. For complete details on the work discussed in this letter, see Fox et al. (2007a, b).

#### References

- Bouché N. et al. 2007, MNRAS 378, 525
- Bouwens R. J. et al. 2004, ApJ 616, L79
- Davé R. et al. 2001, ApJ 552, 473
- Fox A. et al. 2007a, A&A 465, 171
- Fox A. et al. 2007b, A&A, in press, astro-ph/0707.4065
- Gnat O. and Sternberg A. 2007, ApJS 168, 213
- Ledoux C. et al. 2006, A&A 457, 71
- Prochaska J. X. et al. 2005, ApJ 635, 123
- Rauch M. 1998, ARA&A 36, 267
- Wolfe A. M. et al. 2005, ARA&A 43, 861



The diffuse H II region N158 in the Large Magellanic Cloud, first classified by Henize in 1956, is shown in this ESO 2.2 WFI image taken from the 256 M pixel colour image which appeared as ESO PR 50/06. The image size is 13 by 14.5 arcminutes and north is up, east to the left. The superbubble nebula to the north-west (NGC 2081) surrounds the early-type star cluster LH104, identified by Luck and Hodge in 1970. The more compact nebula to the south-west is NGC 2074, also referred to as N158C, which shows signs of recent star formation. There are many young hot stars and Wolf-Rayet stars found across the N158 nebula.